Comparison of Different Strongman Events: Trunk Muscle Activation and Lumbar Spine Motion, Load, and Stiffness

Stuart M. McGill,[1] Art McDermott,[2] and Chad M.J. Fenwick[1]

[1]Department of Kinesiology, University of Waterloo, Waterloo, Canada; and [2]Matrix Strength and Fitness, Andover, Massachusetts

Abstract

McGill, SM, McDermott, A, and Fenwick, CMJ. Comparison of different strongman events: trunk muscle activation and lumbar spine motion, load, and stiffness. *J Strength Cond Res* 23(4): 1148–1161, 2009—Strongman events are attracting more interest as training exercises because of their unique demands. Further, strongman competitors sustain specific injuries, particularly to the back. Muscle electromyographic data from various torso and hip muscles, together with kinematic measures, were input to an anatomically detailed model of the torso to estimate back load, low-back stiffness, and hip torque. Events included the farmer's walk, super yoke, Atlas stone lift, suitcase carry, keg walk, tire flip, and log lift. The results document the unique demands of these whole-body events and, in particular, the demands on the back and torso. For example, the very large moments required at the hip for abduction when performing a yoke walk exceed the strength capability of the hip. Here, muscles such as quadratus lumborum made up for the strength deficit by generating frontal plane torque to support the torso/pelvis. In this way, the stiffened torso acts as a source of strength to allow joints with insufficient strength to be buttressed, resulting in successful performance. Timing of muscle activation patterns in events such as the Atlas stone lift demonstrated the need to integrate the hip extensors before the back extensors. Even so, because of the awkward shape of the stone, the protective neutral spine posture was impossible to achieve, resulting in substantial loading on the back that is placed in a weakened posture. Unexpectedly, the super yoke carry resulted in the highest loads on the spine. This was attributed to the weight of the yoke coupled with the massive torso muscle cocontraction, which produced torso stiffness to ensure spine stability together with buttressing the abduction strength insufficiency of the hips. Strongman events clearly challenge the strength of the body linkage, together with the stabilizing system, in a different way than traditional approaches. The carrying events challenged different abilities than the lifting events, suggesting that loaded carrying would enhance traditional lifting-based strength programs. This analysis also documented the technique components of successful, joint-sparing, strongman event strategies.

Key Words core exercises, lumbar spine, peak activation, strongman events, strength, stability

Address correspondence to Stuart M. McGill, mcgill@healthy.uwaterloo.ca.

23(4)/1148–1161

Journal of Strength and Conditioning Research

Introduction

Strongman events are attracting more interest as training exercises because of their unique demands. No scientific investigation of muscle activation patterns together with estimates of joint loading has been conducted during these events as far as we are aware. Strongman competitors sustain specific injuries, particularly to the back. Thus, we were motivated to quantify spine loading and muscle activation patterns during a variety of strongman events. With the excessive forces observed in this investigation, it is in fact surprising that more athletes are not injured during training and competition. However, as seen in our elite-level subject, innate protective muscle patterns are present to mitigate this possibility. Historically, these events have been limited to television "fringe sports." During the past 5–10 years, however, this unique combination of traditional weight training and more sport-transferable "functional" movements have worked their way into collegiate and even advanced high school weight training programs. This would suggest the importance for understanding the forces generated during the execution of these special events together with their technical demands.

Training for strongmen events has extended to athletes training for other athletic endeavors that require strength. The philosophical foundation for this is that many so-called "functional" training approaches involved natural constraints on the activation of muscle groups. This is because joint torques about the 3 orthopedic axes of each joint must remain in balance to match the task. For example, if the external oblique muscle were needed to create torso twist, the force would also create lateral bend and flexion torques that would have to be offset by other muscles. When training for strength, this need for torque balance and functional "steering" of force through the body linkage creates constraints on activation levels of specific muscles. Despite these constraints, the much higher blood lactate levels measured after maximal pushing and pulling tasks when compared with maximal treadmill running (> 130% higher) demonstrate the supreme physiological demand (1). According to Waller et al. (11), the total body effort surpasses the effort required on training machines and free weights. Thus, it seems that the strongman events are truly unique in a functional sense. They challenge the whole musculoskeletal system in terms of both strength and physiological demand, but they must adhere to the constraints of the tasks involving awkward implements. Clearly, investigation into the mechanics of some of these events should provide insight that will enable performance enhancement and a reduced risk of injury.

It was hypothesized that each event would create a unique challenge to the body, that the Atlas stone lift would create the largest spine compressive load, that the majority of muscle contraction would be to stiffen the spine rather than to create torque, that the tire flip would create the least spinal compressive load, and that the yoke carry would create the highest level of abdominal cocontraction.

Methods

Experimental Approach to the Problem

Normalized and calibrated electromyography (EMG), 3-dimensional spine motion, and external load were recorded, as well as video of both the frontal and sagittal planes of the following events: farmer's walk, super yoke, Atlas stone lift, suitcase carry, keg walk, tire flip, and log lift (see Figure 1). These motion and load data were input into a very anatomically detailed biomechanical model of the torso (3,4,8), which calculated the torso stiffness, compression, and shear loading of the lumbar spine. Stiffness is a necessary precursor of stability; in this case, it was interpreted as a surrogate for column stability.

Subjects

Three healthy men with an average age of 25 years (*SD* 7), average height of 1.76 m (*SD* 0.10), and an average mass of 117.3 kg (*SD* 27.5) participated in this study. All were active competitors in strongman competitions; one was world-class. All subject recruitment and data collection procedures were performed in accordance with the university office of research and ethics guidelines. Also, written informed consent was gained in agreement with *MSSE* and ACSM guidelines.

Procedure

Before instrumentation, the skin over each muscle was shaved and cleansed with a 50/50 H_2O and ethanol solution. Sixteen

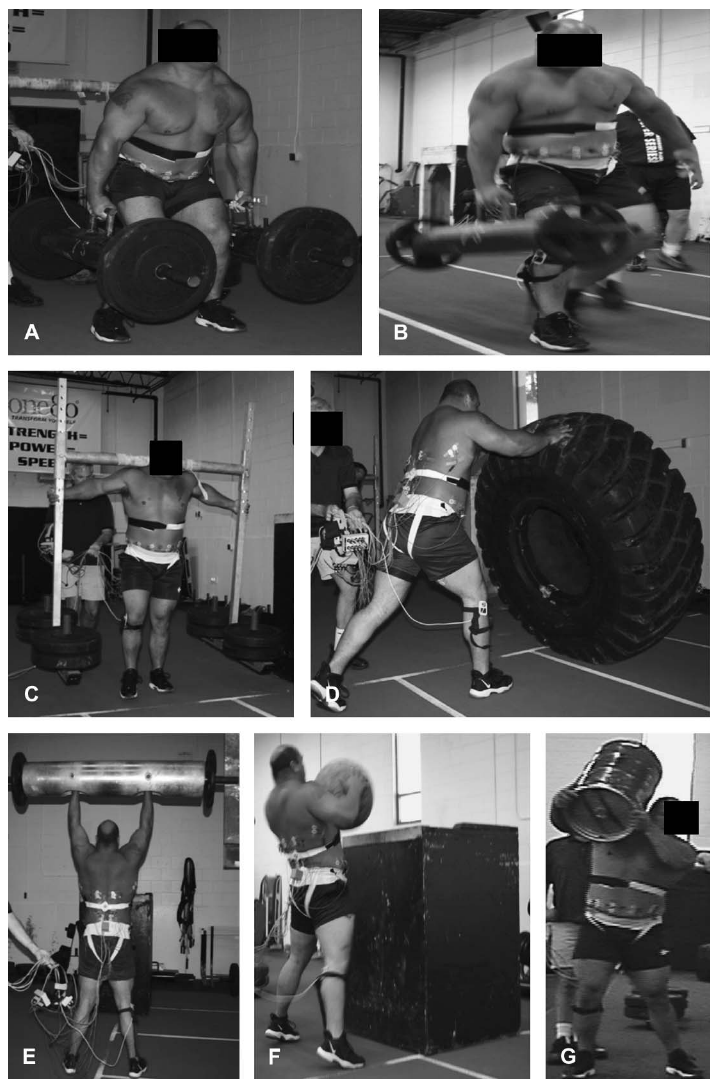

Figure 1. Illustration of the various strongman events performed: A) farmer's walk; B) suitcase carry; C) super yoke walk; D) tire flip; E) log lift; F) stone lift; G) right-shoulder keg walk.

Ag-AgCl surface electrode pairs were placed bilaterally with an interelectrode distance of about 2.5 cm on the following muscles: right and left rectus abdominis (RRA and LRA) lateral to the navel; right and left external obliques (REO and LEO) about 3 cm lateral to the linea semi lunaris but on the same level as the RRA and LRA electrodes; right and left internal obliques (RIO and LIO) caudal to the REO and LEO electrodes and the anterior superior iliac spine and still cranial to the inguinal ligament; right and left latissimus dorsi (RLD and LLD) over the muscle belly when the arm was positioned in the shoulder midrange; right and left upper (thoracic) erector spinae (RUES and LUES) approximately 5 cm lateral to the spinous process (actually longissimus thoracis and iliocostalis at T9); right and left lumbar erector spinae (RLES and LLES) approximately 3 cm lateral to the spinous process (actually longissimus and iliocostalis at L3); right gluteus medius (RGMED) in the muscle belly found by placing the thumb on the ASIS and reaching with the fingertips around to the gluteus medius; right gluteus maximus (RGMAX) in the middle of the muscle belly approximately 4 cm lateral to the gluteal fold; and right rectus femoris (RRF) approximately 5 cm caudal to the inguinal ligament and right biceps femoris (RBF) over the muscle belly midway between the knee and hip. The EMG signals were amplified to produce maximum signals approaching $\pm$ 10 V and then were A/D converted with a 12-bit, 16-channel A/D converter at 2048 Hz.

Each subject was required to perform a maximal contraction of each measured muscle for normalization of each channel (5). For the abdominal muscles, each subject adopted a sit-up position and was manually braced by a research assistant. Each subject then produced a maximal isometric flexor moment followed sequentially by a right and left lateral bend moment and then a right and left twist moment. Little motion took place. For the spine extensors and gluteal muscles, a resisted maximum extension in the Biering Sorensen position was performed (9). A specific RGMED normalizing contraction was also attempted with resisted side-lying abduction (i.e., the clam). Participants laid on their left sides with their hips and knees flexed. Keeping the feet together, each subject abducted his right thigh to parallel, and a research assistant restricted further movement. Normalizing contractions for RRF were attempted, with isometric knee extension performed from a seated position with simultaneous hip flexion on the instrumented side. For RBF, participants laid supine and were instructed to flex the knee and extend the hip, with the researcher manually resisting both movements. The maximal amplitude observed in any normalizing contraction for a specific muscle was taken as the maximum for that particular muscle.

The EMG signals were full-wave rectified and low-pass filtered with a second-order Butterworth filter. A cutoff frequency of 2.5 Hz was used to mimic the EMG to force the frequency response of the torso muscles (2). The EMG signals were normalized to the maximal voluntary contractions to enable physiological interpretation.

Lumbar spine position was measured about the 3 orthopedic axes (flexion/extension, lateral bend, axial twist) using a 3 Space IsoTRAK electromagnetic tracking instrument (Polhemus, Inc., Colchester, Vt). This instrument uses a single transmitter that was strapped to the pelvis over the sacrum and a receiver strapped across the ribcage, over the T12 spinous process. In this way, the position of the ribcage relative to the pelvis was measured (lumbar motion). Spine posture was normalized to that obtained during standing (thus corresponding to 0° of flexion-extension, lateral bend, and twist). For the purposes of describing deviations in spine posture in the Results section, absolute values of the lateral bend and twist angles are reported; thus, the reader knows when participants were more or less laterally bent or twisted during an event. Of course, calculations of spine load incorporated proper polarity in spine posture.

Video was collected at 30 Hz and was interpolated or "up-sampled" to 32 Hz to synchronize with the 3 Space and the EMG data. Cameras were oriented to capture both a sagittal and a frontal plane view.

It was important to measure maximum hip abduction strength to assist in subsequent interpretation of joint moments. Before collection, each participant laid on his left side and abducted his right hip, keeping both legs straight. The abducting force at the ankle during a maximal exertion and length of the moment arm (leg length from greater trochanter to lateral maleolus of the ankle) were measured.

Joint reaction moments were obtained from a linked segment model using hand loads and joint position data as model input (subsequently described).

Description of Strongmen Events

Farmer's walk (FW): In a dead lift position (see Figure 1), each participant held 1 loaded bar (Mastiff Strength Equipment; handle height from ground: 0.43 m) in each hand with a mass of 75 kg each. The load was lifted from the ground, and the participant quickly walked forward several steps and then set the load down.

Left-hand suitcase carry (LHSC): Each participant held 1 loaded bar (see FW for description of the bar used) in his left hands with an average mass of 36.9 kg (*SD* 8). The bar was lifted from the ground, and the participant walked several steps forward and then set the load down.

Right-hand suitcase carry (RHSC): Similar to the LHSC, but the load was in the right hand.

Super yoke walk (YW): A steel yoke (Aluma-Tech; width of crossbar: 1.34 m; mass of yoke unloaded: 43 kg) was loaded with an average total mass of 177.3 kg (*SD* 24.3). In a half-squat position, the yoke bar was placed across each participant's shoulders. Then the participant lifted the yoke from the ground, walked forward approximately 8 m, and set it down.

Keg walk–left shoulder (KWLS): Each participant lifted a beer keg (loaded with sand) with a mass of 40.9 kg from the ground and racked it onto his left shoulder, walked forward several steps, and then set it down.

Keg walk–right shoulder (KWRS): The keg walk was repeated but with the keg placed on the right shoulder.

Log lift (LL): In a dead lift position, each participant lifted a loaded log (Aluma-Tech; log diameter: 0.25 cm; log length: 1.52 m; distance between handles: 0.51 m; mass of log unloaded: 30 kg) with an average total mass of 75.6 kg (*SD* 14.5) and with the handles inside the log in a hammer grip position. The movement consisted of a clean with the log to the shoulder level, a pause, and then an overhead press to full arm extension.

Tire flip (TF): Participants were instructed to flip a large tractor tire (General Tire; model 23.5-25; height of tire when standing: 1.60 m; Width of tire: 0.61 m) with a mass of 309.1 kg, and positioned on its side. Each participant took a deep squat position and hooked his hands under the bottom of the tire. The chest musculature was also "hooked" on the top edge of the tread to transmit upward and forward driving forces. Using a hip hinge, participants drove the tractor tire up and over, keeping arms straight until the end of the TF.

Atlas stone lift (SL): Each participant lifted a large stone (Stone materials: circular poured concrete; stone diameter: 0.43 m) with a mass of 110 kg from the ground to a platform at a height of 1.07 m. This special lift requires the arms and hands to wrap the stone while the spine is curled over the stone. Typically, the stone is lifted and "rolled" onto the thighs, the hands gain new purchase, and the hips extend with the stone "bearhugged." The lift is finished with spine extension as the stone is placed into the pedestal/holder.

Spine Load and Stiffness Estimation

Normalized EMG signals and lumbar spine position data were entered into an anatomically detailed model of the lumbar spine. This model represents approximately 90 muscle lines of action spanning 6 lumbar joints (L5-sacrum to T12-L1). The force and stiffness generated by each muscle fascicle were estimated from a distribution-moment (6) approach, which incorporated muscle activation data (from EMG) together with geometric data (state variables in the model). Then, the measured moment on the low back (from the video film) was compared with the sum of the muscle moment predicted from the distribution-moment model and a gain value assigned to the subject to make a match. In this way, the EMG and subsequent processing was "tuned" for each subject who had unique muscle sizes, geometry, etc. The model tuning task was the LL because external forces were applied just through the log handles, and it was primarily a sagittal plane task. Muscle compressive and shear forces were computed as the summation of the force of all muscle fascicles acting along the anatomic compressive and shear axes, respectively, together with the applied loads of the event, of the L4-L5 joint. For graphic purposes, the absolute values of the shear forces are displayed. Lumbar spine stiffness was computed about each of the flexion/extension and axial twist axes as the average of the rotational joint stiffness (10) estimated across each lumbar joint. Stiffness is a direct correlate of spine stability. A more detailed description of the various components of the modeling techniques can be found elsewhere (4).

The subjects were asked to perform 2 trials of each event. For walking trials, participants were instructed to walk until the research assistant asked them to set the weight down (approximately 10 strides). Because of complications during collection by the difficult tasks observed, the keg walk (both sides) and SL were not statistically analyzed and were analyzed instead as case studies.

Data Analysis

Using the video recorded, each trial (EMG, 3 Space, Force, and Video) was sectioned from the start through to the completion of each strongman event. The start of the event was when the participant was about to lift the load off of the ground, and completion occurred when the load was set back down on the ground.

For each walking event (FW, LHSC, RHSC, YW, KWLS, and KWRS) the frontal plane was digitized with each participant standing on his left leg with the right leg in midswing phase. The hip abduction moment for each walking event was calculated and normalized to the maximum isometric abduction moment-producing capabilities of each subject's hip. For EMG analysis, each walking event (FW, LHSC, RHSC, YW, KWLS, and KWRS) was sectioned into 4 phases to determine the phase of the event at which each muscle reached peak activation. The 4 phases were 1) lift phase, during which where the weight was lifted from the ground to a complete upright position; 2) first step with right leg weight bearing; 3) walking phase; and 4) lower phases, during which the weight was lowered from the upright position to the ground. The phases are illustrated in Figure 2.

A static/quasi-static spine posture was digitized for each subject and event to estimate the external lumbar moment as well as the reaction compression and shear load of the L4/L5 joint. For the FW, LHSC, RHSC, YW, LL, and TF, electromyography, spine position, muscular loading, and stiffness of the lumbar spine were averaged across all 3 subjects, and joint anterior/posterior (A/P) shear and joint compression were calculated from 2 subjects. For the KWLS, KWRS, and SL, electromyography, spine position, muscular loading, and stiffness of the lumbar spine were averaged across 2 subjects only

Statistical Analyses

This study was designed as a series of case studies and not for statistical analysis. Nonetheless, some analysis was conducted and some significance was found. Electromyography, spine position, and spinal/muscular loading were individually analyzed using a 1-way repeated-measures analysis of variance (ANOVA; within factor: exercise; 3 levels; $\alpha = 0.05$), followed by a least squared means post hoc analysis in which a significant main effect as well as interaction differences were found.

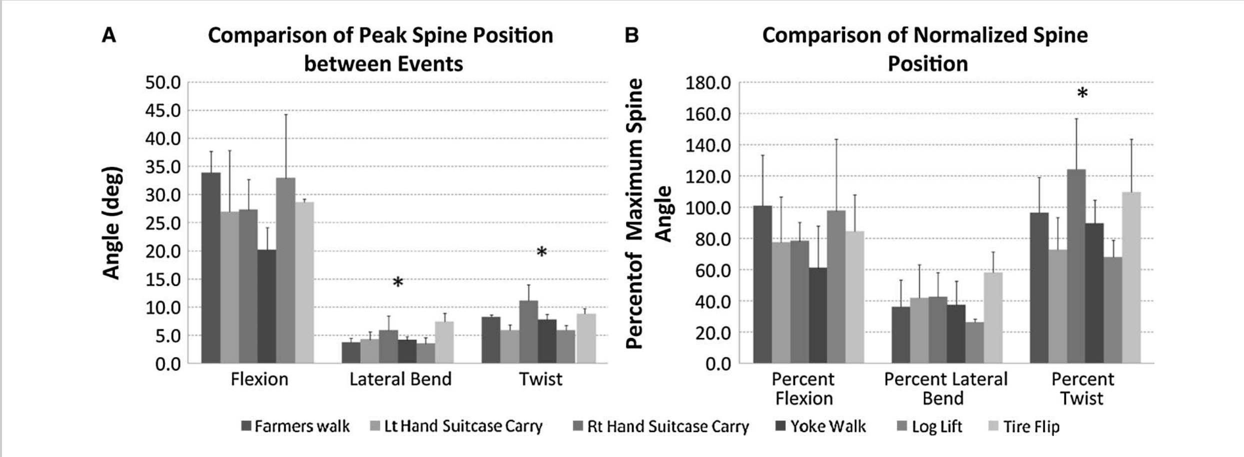

Figure 2. A comparison of the strongman events performed (farmer's walk, right-hand suitcase carry, left-hand suitcase carry, super yoke walk, log lift, and tire flip) in terms of (A) the average measured peak raw lumbar spine angle and (B) normalized spine angle (to the maximum spine range of motion). On average, the super yoke walk was the most spine-conserving event (especially in the flexion axis), whereas the lifting events (log lift and tire flip) elicited larger flexion angles, and the single-handed walking events (mainly the right-hand suitcase carry) produced the larger spine twist angles. This was attributable to the "waddling" gait style. *Statistically significant difference.

A log transform was used to normalize the data because of the small sample size. The log transform reduced some of the inflated means (large range and *SD* within the means) and produced a normal distribution. However, the results are reported as the actual mean values calculated.

Results

Note that 100% MVC was obtained during isometric maximal efforts. Greater than 100% of this MVC is often seen when dynamic motion occurs. Also note that the subjects will be referred to as #1 (the world-class competitor), #2 (who is a state champion), and #3 (who is a local competitor). Thus, they are ranked in descending order of performance and skill.

Global Results

Low-back compression and shear forces (subject average), together with the flexion/extension moment, are listed in Table 1. Compressive forces purely attributable to the muscle forces are listed separately to illustrate the muscle activity to stiffen the spine rather than to just support the reaction moment. For example, subject #1 chose to activate the stiffening muscles to the highest degree in the FW even though the load carried was the same as that carried by other competitors. The compressive force from the muscle forces was 8020 N, and the total compression (including the implement weight and the upper body) on the low back was more than 12 kN. On average, the YW created the highest back compression, which was mainly attributable to torso muscle cocontraction. Of the lifts, the TF produced slightly higher compression on the back than the LL. Note that the leg lift joint compression was slightly lower than the muscle forces acting to compress the spine. This is because the hips were higher than the shoulders actually creating low-back tension. Surprisingly, the SL generated the lowest compression of the 3 lifts because the strongmen curved their torsos over the stone, getting its center of mass closer to their low backs. Also, this technique "hooked" the torso around the stone to aid contact grip. The stone was then "rolled" up the thighs onto the belly before the extension heave onto the platform. However, the SL also produced the largest spine flexion angle. On average, this was more than 140% of the passive spine flexion measured during simply slumping over in the "rag doll" position. Muscle activation throughout the lifting and walking phases of the events is documented in Tables 2 and 3 together with the case study time history figures. Muscle activation levels revealed that the largest gluteal activity occurred during the SL, as did the quadriceps, the upper erector spinae, and many of the abdominal muscles. This TF required the highest activation levels in one latissimus dorsi, the lower lumbar erector spinae, and the hamstrings. These maximum muscle activation levels occurred in different phases of each event, as noted in Table 3. For example, in the FW the abdominal muscles were more apt to peak during the walk, whereas the low-back erector spinae peaked during the lift. Average spine postures and muscular (stiffing) contributions to spine compression are summarized in Tables 2 and 3, but they will be described subsequently for each event.

Comparison of Events

Muscle Activation. See Table 2 for average peak muscle activation levels recorded from all muscles during each strongman event. Even though this study was not designed for rigorous statistical analysis, significant differences were observed and are reported here.

TABLE 1. Average external moment about the lumbar spine, muscular and joint compression and anterior/posterior (A/P) shear, and average masses of the loads lifted in each hand.

		L4/L5 moment	Muscular		Joint		Mass of load lifted (kg)	
			Compression	A/P shear	Compression	A/P shear	Right hand	Left hand
FW	Average	63	7150	−2519	9876	−2409	75	75
	SD	37	2707	1005	3740	1494	0	0
LHSC	Average	61	5492	−1598	6890	−1520		38
	SD	37	1242	363	1804	535		9
RHSC	Average	48	7303	−2376	9061	−2143	42	
	SD	24	2531	887	2740	1163	12	
YW	Average	104	8020	−1894	12043	−1341	91	91
	SD	47	2631	149	2500	206	12	12
LL	Average	351	7287	−2223	7270	−1021	39	39
	SD	94	1085	528	843	437	8	8
TF	Average	792	7061	−2056	7921	−138	155	155
	SD	58	1562	243	1592	331	0	0
SL	Average	183	5690	−1507	5659	−635	27	27
	SD	177	3904	1548	5752	1365	24	24
KWLS	Average	267	6832	−1603	8412	−913	35	35
	SD	127	3453	2941	3762	3221	10	10
KWRS	Average	431	6909	−2737	6591	−1249	100	100
	SD	70	462	106	434	55	0	0

Compression for the muscles alone is listed separately to reveal that muscle forces are the primary source of spine compression. Values for the FW, LHSC, RHSC, YW, KWLS, and KWRS were collected during walking, and values for the LL, TF, and SL were collected during the lifting phase. FW = farmer's walk; LHSC = left-hand suitcase carry; RHSC = right-hand suitcase carry; YW = super yoke walk; LL = log lift; TF = tire flip; SL = Atlas stone lift; KWLS = keg walk–left shoulder; KWRS = keg walk–right shoulder.

The RRA activation level recorded during the TF was significantly higher than that recorded during LL, YW, LHSC, FW, and RHSC, whereas the LL and YW elicited higher activation than the RHSC ($F = 5.83$, $p = 0.0089$). Similarly, the TF produced significantly larger activation of the REO muscle than the LL, FW, and RHSC events did, whereas the LHSC, YW, LL, and FW elicited significantly greater levels of muscle activation than the RHSC did ($F = 4.87$, $p < 0.0162$). Again, the TF event elicited the highest activation of the LEO muscle, which was significantly larger than the FW and LHSC, whereas the RHSC, LL, YW, and FW elicited activation levels that were significantly higher than that recorded during the LHSC ($F = 7.67$, $p = 0.0033$). Activation levels of the RLD muscle recorded during the TF were significantly larger than that recorded during the RHFW, LHSC, and YW, whereas the FW even produced activation levels significantly larger than the LHSC and YW, and the LL and RHSC produced higher activation levels than the YW did ($F = 5.71$, $p = 0.0096$). The activation level of the LLD muscle during the TF was significantly higher than during the LHSC, RHSC, and YW events, whereas significantly higher activations were observed during the FW and LL than during the RHSC and YW events ($F = 5.30$, $p = 0.0123$). During both the LL and TF events, the peak activation of the RUES muscle observed was significantly higher than that observed during the RHSC and LHSC, whereas the FW, YW, and RHSC events produced significantly higher peak activation than the LHSC did ($F = 6.83$, $p = 0.0051$). Similarly, the LL event produced significantly higher activation of the LUES than the YW, LHSC, and RHSC did, whereas the peak activation during the TF was significantly higher than during the LHSC and RHSC, and larger activations were observed during FW and YW events than during the RHSC ($F = 8.08$, $p = 0.0028$). Peak activation of the RLES muscle during the performance of the TF was significantly higher than during the YW, LHSC, and RHSC, whereas the peak activation observed during the LL, FW, YW, and LHSC was significantly higher than the activation observed during the RHSC ($F = 9.29$, $p < 0.0016$). The LLES muscle showed significantly higher activation during the TF compared with the YW, RHSC, and LHSC, whereas significantly higher activation was observed during the FW, LL, YW, and RHSC events than during the LHSC event ($F = 7.79$, $p < 0.0032$). The TF event produced significantly higher activation of the RBF muscle than the FW, RHSC, and LHSC did, whereas the LL, YW, FW, and RHSC events produced significantly higher activation than the LHSC did ($F = 8.30$, $p = 0.0025$). The TF event elicited significantly higher activation of the RRF muscle than the FW, RHSC, and LHSC events did, whereas activation levels

Table 2. Average peak muscle activation for the trunk and selected hip and thigh muscles recorded during all strongman events (the case study of the KWRS, KWLS, and SL are included).

Event		Muscle															
		RRA	LRA	REO	LEO	RIO	LIO	RLD	LLD	RUES	LUES	RLES	LLES	RGMED	RGMAX	RBF	RRF
FW	Mean	13.3	20.6	50.4	39.3	110.8	80.9	151.7	169.2	91.4	77.6	143.5	105.8	108.4	114.1	54.0	77.4
	SD	3.8	12.6	17.4	30.6	33.0	26.9	26.7	55.4	54.7	29.3	36.7	51.1	66.9	70.3	13.7	35.6
RHSC	Mean	5.6	21.2	29.0	61.5	62.6	47.3	91.4	68.9	52.1	32.4	44.1	77.4	57.3	50.5	48.3	56.5
	SD	1.8	14.6	17.8	21.9	26.8	45.3	39.1	23.2	17.3	4.6	9.1	21.3	23.6	31.2	8.6	11.4
LHSC	Mean	14.6	6.3	65.1	12.6	51.9	31.5	65.3	97.4	24.9	47.1	96.9	31.6	64.1	78.2	31.2	41.1
	SD	4.5	2.2	24.4	5.3	41.5	4.6	6.2	55.7	17.6	6.2	20.4	10.1	38.7	39.5	7.5	9.2
YW	Mean	22.3	32.5	58.8	47.5	128.3	52.6	45.5	51.9	65.6	69.3	107.4	79.2	108.1	113.0	61.7	106.9
	SD	18.1	22.7	29.1	31.7	21.7	40.8	31.7	26.4	14.4	17.5	31.5	10.2	69.7	52.1	6.3	23.5
LL	Mean	27.3	29.1	61.5	49.6	98.1	91.3	146.2	179.7	128.0	135.7	161.7	93.0	156.1	157.6	73.2	100.2
	SD	27.8	12.4	49.1	27.9	44.0	30.6	90.8	102.2	87.6	87.0	92.8	37.6	163.9	147.1	26.4	69.5
TF	Mean	87.8	69.3	106.6	80.5	141.5	97.6	227.2	237.8	118.1	100.3	236.2	157.7	179.8	200.4	90.7	154.5
	SD	63.9	70.6	45.4	12.2	54.6	34.1	145.4	84.1	47.2	21.1	72.2	31.0	75.6	61.5	7.2	86.2
KWLS	Mean	30.5	45.6	73.6	87.0	105.4	85.3	57.1	108.1	102.3	72.2	114.3	84.6	87.5	64.5	70.0	53.4
	SD	14.8	42.8	62.2	46.0	14.3	36.9	35.4	17.4	67.3	36.8	26.5	16.3	31.9	7.0	25.8	29.4
KWRS	Mean	19.9	23.2	64.9	39.7	96.4	79.1	49.4	102.2	91.4	76.2	138.7	92.6	131.7	89.7	75.2	72.0
	SD	1.7	6.4	21.4	17.7	11.3	20.2	20.1	15.7	29.5	46.0	29.2	35.9	0.3	24.5	22.5	40.6
SL	Mean	77.6	76.8	97.6	103.6	102.0	117.5	109.3	148.9	131.8	154.7	226.0	137.3	288.6	259.1	85.4	176.8
	SD	41.6	24.7	67.7	2.5	63.0	67.3	37.5	58.6	77.1	36.4	81.0	30.9	131.6	154.9	7.8	52.1

FW = farmer's walk; RHSC = right-hand suitcase carry; LHSC = left-hand suitcase carry; YW = super yoke walk; LL = log lift; TF = tire flip; KWLS = keg walk–left shoulder; KWRS = keg walk–right shoulder; SL = Atlas stone lift; RRA = right rectus abdominis; LRA = left rectus abdominis; REO = right external oblique; LEO = left external oblique; RIO = right internal oblique; LIO = left internal oblique; RLD = right latissimus dorsi; LLD = left latissimus dorsi; RUES = right upper (thoracic) erector spinae; LUES = left upper (thoracic) erector spinae; RLES = right lumbar erector spinae; LLES = left lumbar erector spinae; RGMED = right gluteus medius; RGMAX = right gluteus maximus; RBF = right biceps femoris; RRF = right rectus femoris.

TABLE 3. The number of times a muscle reached peak activation during a specific phase of each strongman event; each phase is illustrated in Figure 2 and is listed as follows: 1) lifting phase, 2) first step with right leg weight bearing, 3) walking phase, and 4) lowering phase.

	Muscle															
	RRA	LRA	REO	LEO	RIO	LIO	RLD	LLD	RUES	LUES	RLES	LLES	RGMED	RGMAX	RBF	RRF
FW																
Lift	1	1	1	0	1	1	4	4	3	4	5	4	2	3	3	1
First step	0	1	0	1	0	0	0	0	0	0	0	1	3	2	1	0
Walk	4	3	4	4	4	4	0	1	0	0	0	0	0	0	1	4
Lower	0	0	0	0	0	0	1	0	2	1	0	0	0	0	0	0
LHSC																
Lift	0	1	1	3	2	3	0	4	3	2	4	4	5	1	0	1
First step	0	1	2	1	1	0	2	0	2	0	1	0	0	3	0	0
Walk	5	3	2	1	2	2	3	0	0	0	0	0	0	1	5	3
Lower	0	0	0	0	0	0	0	1	0	3	0	1	0	0	0	1
RHSC																
Lift	1	0	3	0	3	2	4	3	4	5	5	5	2	3	1	4
First step	1	0	1	0	1	0	1	1	1	1	1	1	3	3	2	0
Walk	4	5	2	6	2	3	0	1	0	0	0	0	0	0	3	2
Lower	0	1	0	0	0	1	1	1	1	0	0	0	1	0	0	0
YW																
Lift	0	0	0	0	0	1	1	2	3	5	4	4	2	2	0	1
First step	1	0	0	1	1	1	1	0	0	0	0	0	1	1	1	1
Walk	4	5	5	4	4	3	1	2	0	0	1	1	2	2	4	3
Lower	0	0	0	0	0	0	2	1	2	0	0	0	0	0	0	0
KWLS																
Lift	1	1	2	2	2	2	2	2	2	2	2	2	2	2	2	1
First step	1	1	0	0	0	0	0	0	0	0	0	0	0	0	0	0
Walk	0	0	0	0	0	0	0	0	0	0	0	0	0	0	0	1
Lower	0	0	0	0	0	0	0	0	0	0	0	0	0	0	0	0
KWRS																
Lift	1	1	1	1	0	1	1	1	2	2	2	2	2	2	2	1
First step	1	1	1	1	1	0	0	0	0	0	0	0	0	0	0	0
Walk	0	0	0	0	0	0	1	1	0	0	0	0	0	0	0	1
Lower	0	0	0	0	1	1	0	0	0	0	0	0	0	0	0	0

Three lifters performed 2 trials in total, but, on occasion, technical difficulties compromised 1 trial, which was not analyzed.

FW = farmer's walk; LHSC = left-hand suitcase carry; RHSC = right-hand suitcase carry; YW = super yoke walk; KWLS = keg walk–left shoulder; KWRS = keg walk–right shoulder; RRA = right rectus abdominis; LRA = left rectus abdominis; REO = right external oblique; LEO = left external oblique; RIO = right internal oblique; LIO = left internal oblique; RLD = right latissimus dorsi; LLD = left latissimus dorsi; RUES = right upper (thoracic) erector spinae; LUES = left upper (thoracic) erector spinae; RLES = right lumbar erector spinae; LLES = left lumbar erector spinae; RGMED = right gluteus medius; RGMAX = right gluteus maximus; RBF = right biceps femoris; RRF = right rectus femoris.

during the YW event were significantly higher than during the RHSC and LHSC events, and the LL event was significantly higher than during the LHSC ($F = 5.65$, $p = 0.0099$). Peak activation of the RGMAX muscle during the TF event was significantly higher than the levels produced during the YW, FW, LHSC, and RHSC events, whereas the LL produced significantly higher activation than both the LHSC and RHSC did, and the peaks during the YW and FW events were significantly higher than that during the RHSC ($F = 5.98$, $p = 0.0082$). The TF event produced peak activation levels in the RGMED muscle that were significantly higher than those produced during the YW, FW, LHSC, and RHSC, whereas the peak muscle activation levels during the LL, YW, and FW events were significantly larger than during the RHSC event ($F = 7.01$, $p = 0.0047$). There were no significant differences in the activation levels of the internal obliques and LRA muscles between the events performed.

Spine Posture. During the TF event, significantly larger lateral bend angles were observed compared with the angles observed during the YW, LHSC, FW, and LL events ($F = 3.64$, $p = 0.0390$). However, when analyzing the corresponding normalized spine angle, no statistical differences were found.

Peak twist angle recorded during the RHSC was significantly larger than the angle measured during the FW, YW, LL, and LHSC, whereas the angles measured during the TF, FW, and YW events were significantly larger than during the LL and LHSC events ($F = 10.92$ $p = 0.0008$). When peak spine angle was normalized, the RHSC event was significantly larger than the YW, LHSC, and LL events, whereas the TF event was significantly larger than the LHSC and LL ($F = 6.62$, $p = 0.0057$). A summary of raw and normalized spine position is illustrated in Figure 2.

Muscular Loading and Stiffness of the Lumbar Spine. The muscular compression of the lumbar spine measured during the TF event was significantly larger than the compression measured during the RHSC and LHSC, whereas the lumbar compression levels measured during the YW, FW, and LL events were significantly higher than during the LHSC ($F = 5.16$, $p = 0.0134$; see Figure 3).

The TF, FW, and LL events challenged the torso flexion extension musculature significantly greater than the RHSC and LHSC events did, whereas the YW event required significantly larger muscular stiffness in the flexion/extension axis than did the LHSC event ($F = 6.54$, $p = 0.0060$).

The TF, FW, and LL events challenged the axial twist capabilities of the torso musculature significantly more than the LHSC event did ($F = 3.35$, $p = 0.0492$)

Summary of Each Strongman Event

Farmers Walk. During the first trial of the FW event, all participants lead with the left foot (right leg standing), whereas during the second trial all participants lead with the right foot (left leg standing). Peak activation of the abdominals and RRF muscle occurred during the walking phase; however, peak activation of the latissimus dorsi, thoracic, and lumbar erector spinae muscles occurred during the lifting phase of the event. For the #3 strongman, the RGMED muscle reached peak activation during the lift, whereas for the more competitive strongmen, peak activation of the RGMED occurred during the first step. Strongman #1 reached peak activation of the RGMED muscle while he was standing on his left leg. This most skilled strongman lifted the load off the ground and then ballistically threw his right leg up to take his first step. The RBF muscle was challenged the most during the first step and walking phases, except during 1 trial, in which case 1 participant elicited peak activation during the lift phase (Tables 2 and 3).

Peak lumbar spine flexion angle occurred during the lifting phase of the event, peak lateral bend angle followed no trend, and peak twist occurred during the first step phase of the FW event. The average peak lumbar spine flexion, lateral bend, and twist angles were 33.9° (*SD* 3.8), 3.6° (*SD* 0.8), and 8.2° (*SD* 0.4), respectively, which correspond to 100.8% (*SD* 32.3), 36.1% (*SD* 17.3), and 96.4% (*SD* 22.4) of the total normalized lumbar spine range of motion (see Figure 2).

Peak muscular A/P shear, compression, and stiffness in the flexion/extension axis occurred during the lifting phase of the FW event, whereas the medial/lateral (M/L) shear force peaked during the first step and walking phases. Peak muscular stiffness in the lateral bend axis occurred in either the lifting phase or the walking phase (Figure 3).

The load in both hands produced a hip abduction moment that was, on average, 97.2% (*SD* 27.8) of the participants normalized to the maximum hip abduction moment measured during the controlled hip abduction effort. Whereas subject #1 was not at his maximum load, the maximum hip abduction strength for subject #3 was 231 N·m, yet more than 264 N·m was needed to complete the task. This mechanism will be described in the Discussion section.

Left-Hand Suitcase Carry. During the LHSC, all participants made their first step with their left leg standing and right leg

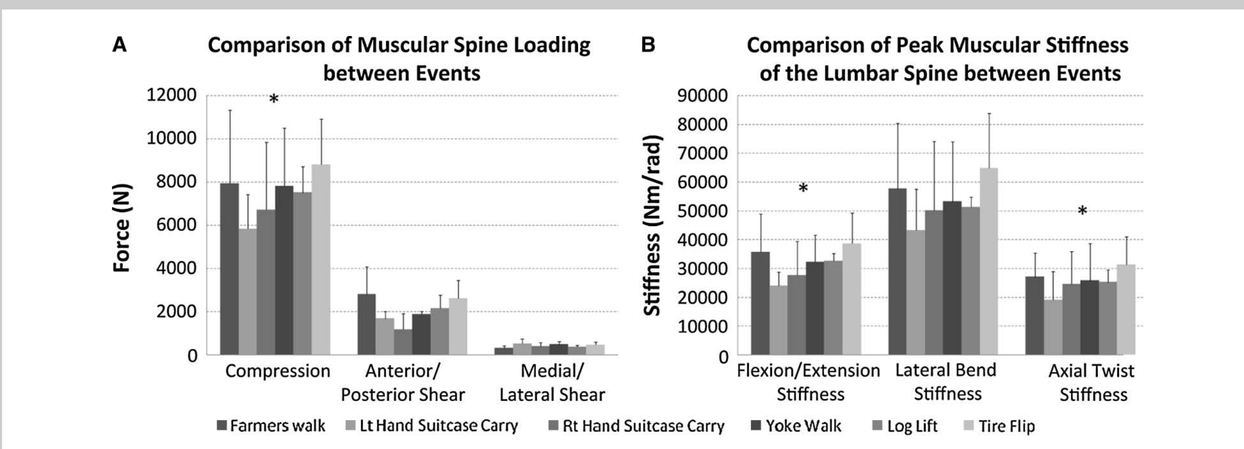

Figure 3. A comparison of muscular compressive spine load (A) and stiffness of the L4/L5 joint representing the lumbar spine. This compression and stiffness ensure spine stability, which was sufficiently high in all events. Note that this was not the total spine compression. *Statistically significant difference.

swinging forward. The RRA, REO, LRA, RLD, RBF, and RRF muscles reached peak activation during either the first step phase or the walking phase, whereas the left oblique muscles reached peak activation during the lifting phase. During 2 trials, the RIO muscle peaked during the lifting phase and in 2 trials during the walking phase. The LLD and the right and left back muscles reached peak activation during the lift or lowering phases of the event. The RGMED and RGMAX muscles peaked during the lift or first step (with the right leg weight bearing) phases.

Average peak flexion occurred during the lifting and lowering phases of the LHSC event, whereas average peak lateral bend occurred during the walking phase with 1 trial during the lifting and lowering phases each. Peak twist angles of the lumbar spine did not reveal a trend, being spread out over the 4 phases. The average peak spine flexion, lateral bend, and twist angles were 27.0° (*SD* 10.9), 4.2° (*SD* 1.4), and 5.8 (*SD* 0.9), which correspond to 77.4% (*SD* 29.2), 41.8% (*SD* 21.3), and 72.7% (*SD* 20.5) of the normalized total spine motion.

Average peak muscular A/P shear, compression, and muscular stiffness of the lumbar spine in the flexion/extension axis occurred during the lifting phase of the LHSC event, whereas the M/L shear force peaked in various phases. Peak muscular stiffness in the lateral bend and the axial twist axis occurred across the lifting/first step/walking phases and did not show a real trend. Average muscular posterior shear, compression, and M/L shear were 1672 N (*SD* 326) in the posterior direction, 5841 N (*SD* 1565) of compression, and 521 N (*SD* 218), respectively. The average peak muscular stiffness of the lumbar spine was highest about the lateral bend axis.

The suitcase event required 87.6% (*SD* 10.69) of the normalized maximum total isometric hip abduction capabilities. Note that the RHSC was a mirror image of the LHSC.

Super Yoke Walk. The abdominal and thigh muscles reached peak activation during the walk or first step phases of this event. Peak activation of the thoracic and lumbar erector spinae muscles occurred during the lifting and lowering phases of this event, with few exceptions. The RLD and LLD muscles varied in the phase at which they reached peak activation. Peak activation of the RGMED and RGMAX varied across the lift, walk, and first step phases.

Peak spine flexion of the lumbar spine was observed primarily during the lowering phase, whereas peak lateral bend and twist angles were observed during the walk phase.

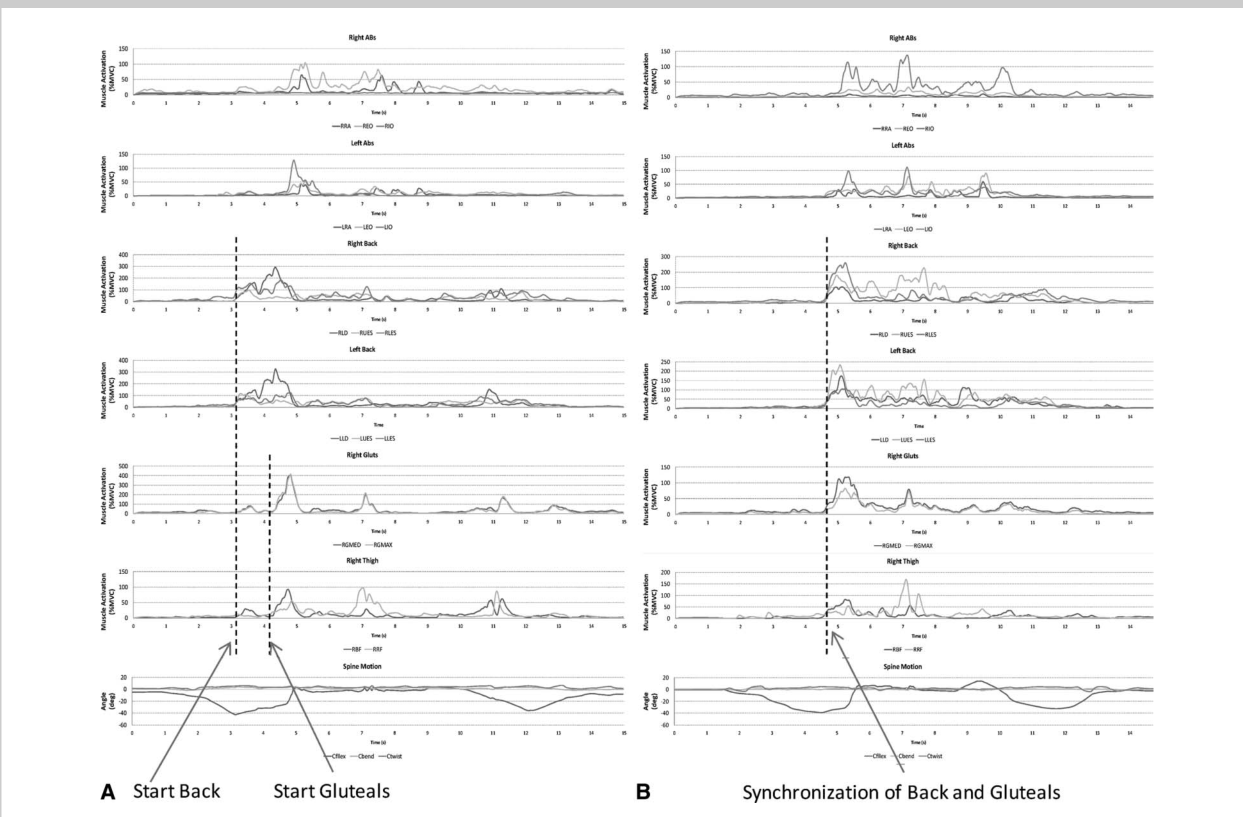

Figure 4. This time history shows that during a poorly performed log lift (A), the back muscles are activated and the log moves without corresponding gluteal activity. The better log lift performance (B) shows simultaneous contraction of the back and gluteal muscles.

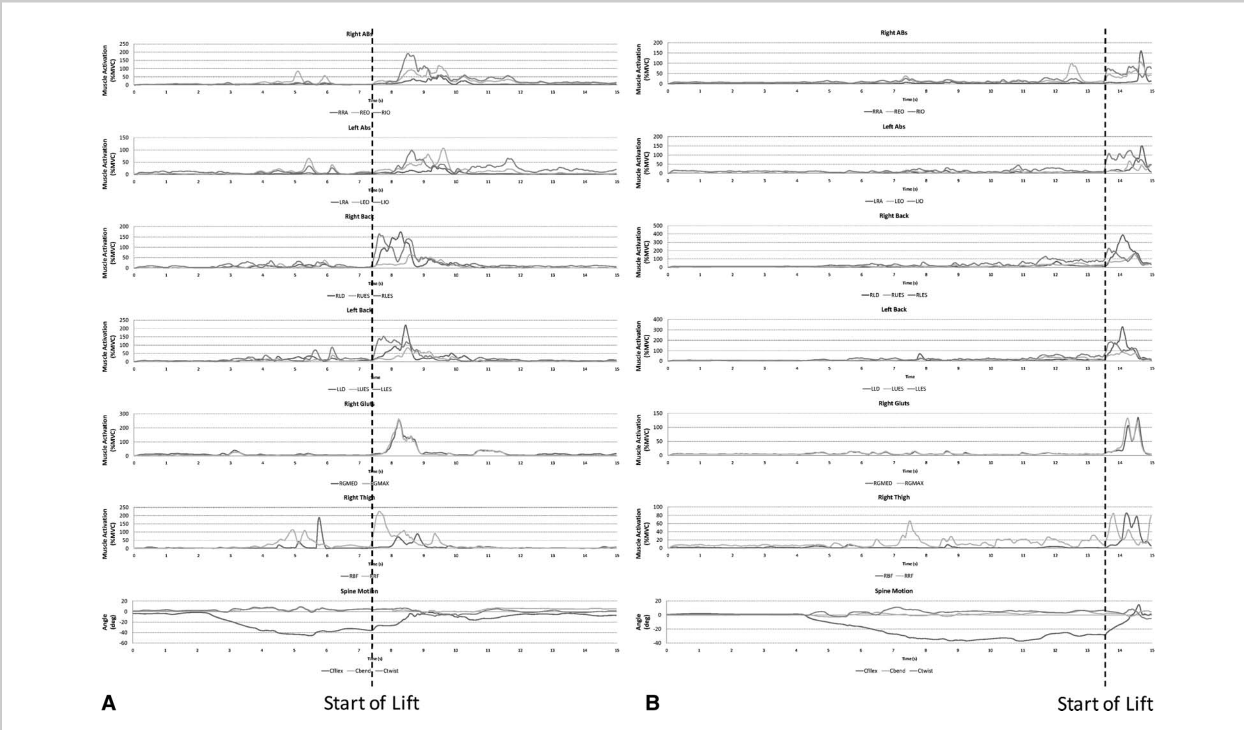

Figure 5. During a poor performance of the tire flip (A), the participant lacks a sufficient abdominal brace at the beginning of the event and has lagging gluteal activation. For the better tire flip strategy (B), the participant braces his abdominals and then begins the flip with a more explosive exertion. The vertical lines note the start of the lift.

The average peak spine flexion, lateral bend, and twist angles were 20.2° (*SD* 3.9), 4.1° (*SD* 0.6), and 7.7° (*SD* 1.0), respectively, which correspond to 60.9% (*SD* 26.8), 37.3% (*SD* 15.2.9), and 89.6% (*SD* 15.0) of the total normalized spine range of motion.

Peak muscular A/P shear and compression forces, along with muscular stiffness in the flexion extension axis acting on the L4/L5 joint, occurred during the lifting phase of the event. The M/L shear occurred primarily during the walking phase, whereas peak muscular stiffness in the lateral bend and axial twist axes occurred during either the lift or walk phases.

The mass of the yoke produced a hip abduction moment that was, on average, 112% (*SD* 39.2) of the participants' normalized hip abduction moment strength measured during the controlled maximum hip abduction effort. For example, subject #2 was measured to be able to produce 271 N·m of maximal hip abduction strength. However, during some strides, 457 N·m of hip abduction torque were required, but the task was successful because of torso stiffening.

Keg Walk–Left Shoulder. During the KWLS event, most muscles reached peak activation during the lifting phase of the event; however, the rectus abdominis of 1 subject reached peak activation during the first step phase, and the RRF muscle peaked during the walking phase. Average peak muscle activation levels for all muscles observed during the KWLS can be found in Table 2.

During the KWLS event, the peak flexion angle was observed during the lifting phase, and the peak twist angle occurred during the first step phase; for 1 subject, peak lateral bend occurred during the lifting phase, whereas the other subject peaked during the walking phase. See Table 3 for the number of trials in which peak spine angle occurred during a specific phase of the event. Average peak lumbar flexion, lateral bend, and twist angles during the KWLS event were 28.3° (*SD* 4.6), 7.7° (*SD* 1.2), and 9.6° (*SD* 3.9), respectively, which correspond to 94.4% (*SD* 33.7), 89.7% (*SD* 26.9), and 107.8% (*SD* 1.4) of their normalized maximum ranges of motion in the 3 axes, respectively.

When performing the KWLS, peak muscular A/P shear and compression, along with muscular stiffness of the lumbar spine in the lateral bend, axial twist, and flexion/extension axis, were observed during the lifting phase. Muscular posterior shear, compression, and M/L shear forces acting on the L4/L5 joint were 2382 N (*SD* 442), 7754 N (*SD* 2218), and 399 N (*SD* 216), respectively. Average peak muscular stiffness of the lumbar spine in the flexion/extension, lateral bend, and axial twist axis were 33217 N·m·rad^{-1} (*SD* 10655), 61150 N·m·rad^{-1} (*SD* 25579), and 27021 N·m·rad^{-1} (10735), respectively. These numbers indicate a relative stiffness for

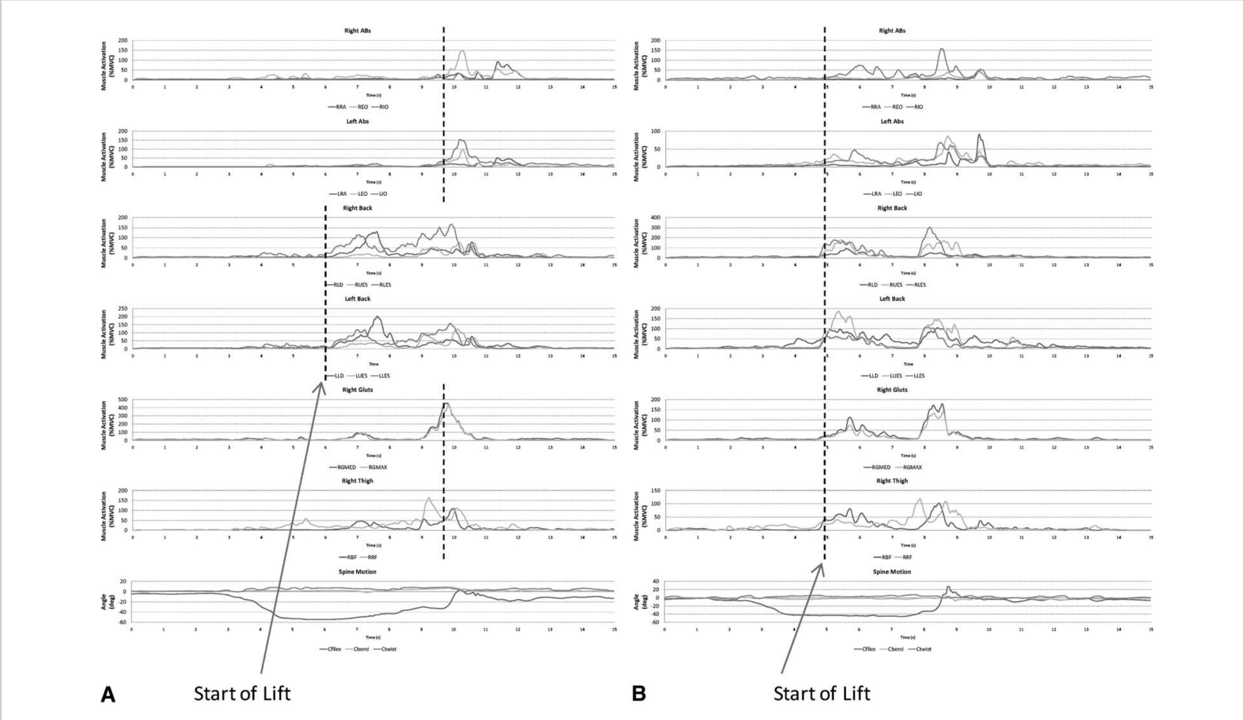

Figure 6. During a poor performance of the stone lift (A), the participant lifts entirely with his back muscles. The lifter using better technique (B) integrates his back muscles with the abdominal and gluteal muscles to stiffen and lift the stone. Note that the spine does not move in extension until the final extension drive to place the stone on the pedestal.

comparison with other events about the same axis. For example, a value about 1 axis cannot be compared with a value about another axis. Simply, a larger number about 1 axis means more stiffness and stability.

The abduction moment created by the mass of the keg acting on the hip during the KWLS event required 36.1% (*SD* 3.8) of the normalized hip abduction capabilities measured during the maximum isometric hip abduction effort.

Log Lift. Average peak muscle activation for all muscles observed during the LL is presented in Table 2. Average peak lumbar spine flexion, lateral bend, and twist were 32.9° (*SD* 11.3), 3.5° (*SD* 1.1), and 5.8° (*SD* 0.9), respectively, and correspond to 97.5% (*SD* 46), 26.3% (*SD* 1.8), and 67.8% (*SD* 10.8) of the normalized maximum spine ranges of motion in the respective 3 axes.

The muscular posterior shear and compression were 2140 N (*SD* 611) and 7501 N (*SD* 1216).

A case study of technique (see Figure 4) illustrates the poor sequencing of muscle activity by the club strongman. He began the lift using his erector spinae without abdominal bracing or sufficient torso stiffness. In addition, there was negligible hip extensor activity until later in the lift. In contrast, the world-class strongman stiffened the torso with abdominal bracing that corresponded to simultaneous back and hip extension, and this was maintained until the log was racked ready for the final overhead press phase.

Tire Flip. When performing the TF, average peak lumbar spine flexion, lateral bend, and twist were 32.9° (*SD* 11.3), 3.5° (*SD* 1.1), and 5.8° (*SD* 0.9), respectively, which correspond to 97.5% (*SD* 46.0), 26.3% (*SD* 1.8), and 67.8% (*SD* 10.8) of the normalized maximum spine ranges of motion in the 3 respective planes.

The muscular posterior shear, compression, and M/L shear of the lumbar spine were 2620 N (*SD* 822), 8812 N (*SD* 2106), and 463 N (*SD* 114), respectively, on average. A case study shows the similar simultaneous coordination of the force abdominals, back, and hip extensors to ensure the "lifter's wedge" exemplified by the world-class strongman; inferior preparation of the stiffening wedge is shown by the less skilled strongman (see Figure 5).

Stone Lift. When performing the SL, the average peak lumbar spine flexion, lateral bend, and twist were 49.9° (*SD* 7.0), 7° (*SD* 1.3), and 7.7° (*SD* 1.7), respectively, which correspond to 146.1% (*SD* 31.5), 54.4% (*SD* 11.4), and 102.7% (*SD* 9.4) of the normalized maximum spine ranges of motion in the 3 respective planes of motion.

Muscular posterior shear, compression, and M/L shear acting on the lumbar spine were 2736 N (*SD* 104), 6908 N

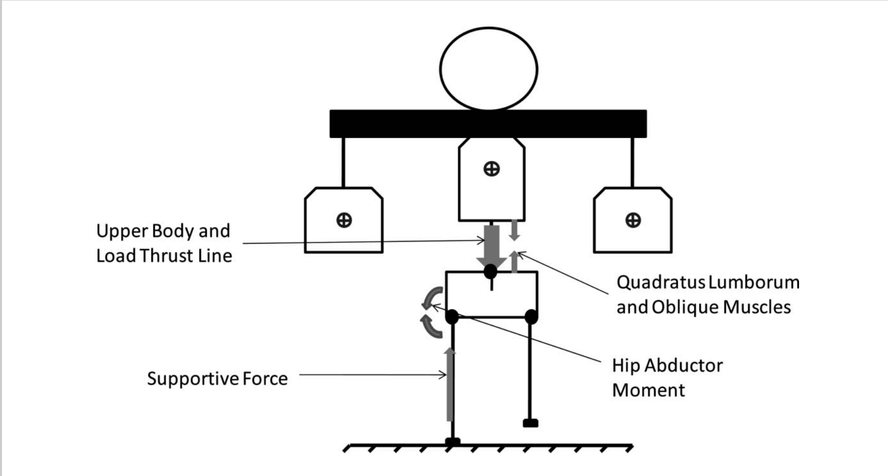

Figure 7. Strongman competitors require more hip abduction strength to perform the carrying/walking tasks than the hip is capable of producing. They find an alternate source of strength by the braced torso musculature, which lifts the pelvis to allow leg swing and leg support. Short, rapid steps allow this mechanism to work.

(*SD* 539), and 376 N (*SD* 82), respectively. This level of compression is quite modest when compared with other events. The case study (Figure 6) shows how the spine is fully flexed and remains flexed for the majority of the lift. The spine is "hooked" over the stone and remains hooked as the stone is rolled up to the thighs. The extension of the hip and spine is used to place the stone on the platform. The world-class strongman once again used total torso stiffening to lock the spine, whereas the club strongman moved the spine and had distinct phases in muscle activation, compromising both performance and protective stiffness.

Discussion

The various strongman events create challenges to different parts of the body in terms of load and athleticism. Although it had been hypothesized that the SL would create the highest compressive load on the lumbar spine, this was not the case. The stone's center of mass was positioned close to the low back by the strongman, who curled over the stone with a torso "hooking" technique. This required extreme spine flexion, which was maintained until the final hip and torso extension thrust to place the stone on the platform. The hypothesis that the majority of spine load was from muscle activity used to stiffen the spine was certainly true for the walk and carry events. The YW, for example, generated the highest spine compression that resulted from the bracing action of the torso musculature to support the yoke load (and to buttress the strength-deficient hip, as discussed in the next paragraph). The lifting components of the events, not surprisingly, generated high spine compression associated with spine extensor torque generation.

The world-class strongman demonstrated much better techniques both for performance enhancement and injury risk reduction. During the lifting components, he coordinated hip extension with torso stiffness, which was accomplished with abdominal and extensor muscle bracing. This was employed just before the extension effort, which, in some cases, was explosive. The less accomplished strongmen (#2 and #3) failed to generate this "lifter's wedge"; either their torso musculature or hips were engaged too late in the lift. This not only created an energy leak through the linkage but also produced more spine load—they used their back muscles rather than hip extensor torque to move the core linkage. Also interesting was ability of the strongmen to generate spine and pelvis stability with torso stiffness during the carry events. For example, in the YW, the load down through the spine requires an extreme hip abduction torque to lift the pelvis and allow the opposite leg to lift and perform the swing phase of the walking cycle. The abduction hip torque needed to lift the pelvis exceeds the abduction strength that we measured in the strongmen. They simply did not have enough hip strength to accomplish the task. Thus, they needed to employ another source of strength. In this case, they braced the torso and lifted the pelvis with lateral torso muscle–the obliques and quadratus lumborum (see Figure 7)–to assist the supporting hip. Interestingly, strongmen often tear or damage the quadratus lumborum. This suggests that strongman events involving asymmetric carries would assist many athletes in training the torso brace and strength to support the hips/pelvis/spine.

The SL is an interesting study for the tradeoff between performance and injury risk control. While the spine is fully flexed to hook over the stone, this assists in getting the stone as close as possible to the low back and hip. These are the joints subjected to the most torque and, therefore, are the limiters of performance (notwithstanding grip on the stone). However, full spine flexion is the posture in which the spine has the lowest tolerance or the highest risk of end-plate fracture (7). However, the spine in the world-class lifter remained in this locked position until the final extension phase needed to place the stone. In this way, spine power was low during the lifting phase (i.e., no spine motion). Low spine power reduces injury risk, and high spine power (both high load and high spine velocity) greatly increases injury risk (7).

There are no data that we could find to compare with the data of this study.

Only 3 strongmen participated in this study, but it seems to be the first to quantitatively investigate the strongman events.

This study was designed as a series of case studies, given the unique demands of the tasks and capabilities of the strongmen, and not for statistical analysis. Nonetheless, statistical significance was found for several variables. In this way, many repeated trials were not conducted to ensure stability of the results. Certainly, the highly skilled strongman had little variability in technique between the 2 trials of lifting events and between multiple strides of carrying events.

Practical Applications

In summary, the majority of the spine load is from the muscles themselves cocontracting to stiffen the torso. Technique differences were observed between the world-class competitor and the others that led to superior stiffness and hip and back moment generation to enhance performance and reduce the risk of injury. Special demands were noted; for example, the very large moments required at the hip for abduction when performing the YW or the single-arm FW exceeded the strength capabilities of the hip. Yet, the task was completed. This makes obvious the importance of muscles such as the quadratus lumborum for the generation of frontal plane torque to support and stiffen the torso/pelvis and assist the strength-deficient hip. Surprisingly, the YW produced the highest compressive loads on the back. This was attributable to the massive torso muscle cocontraction, which produced torso stiffness to ensure spine stability. Strongman events clearly demonstrate the need for substantial torso musculature cocontraction to develop the necessary stiffness to prevent the spine from buckling. In fact, this was seen as a source of strength for weaker joints such as the hip in abduction. Each event challenges the body linkage and the stabilizing system in a different way so that the weak link will be found. The carrying events challenged different abilities than the lifting events, suggesting that carrying would enhance traditional lifting-based strength programs. The data and findings here will help those who are training for strength and stability to make better training choices.

Acknowledgments

We thank the Natural Science and Engineering Research Council of Canada (NSERC) for their financial support.

References

1. Berning, JM, Adams, KJ, Climstein, M, and Stamford, BA. Metabolic demands of junkyard training: pushing and pulling a motor vehicle. *J Strength Cond Res* 21: 853–856, 2007
2. Brereton, LC and McGill, SM. Frequency response of spine extensors during rapid isometric contractions: effects of muscle length and tension. *J Electromyogr Kinesiol* 8: 227–232, 1998.
3. Cholewicki, J and McGill, SM. Lumbar posterior ligament involvement during extremely heavy lifts estimated from fluoroscopic measurements. *J Biomech* 25: 17–28, 1992.
4. Cholewicki, J and McGill, SM. Mechanical stability of the in vivo lumbar spine: implications for injury and chronic low back pain. *Clin Biomech* 11: 1–15, 1996.
5. Kavcic, N, Grenier, S, and McGill, SM. Quantifying tissue loads and spine stability while performing commonly prescribed low back stabilization exercises. *Spine* 29: 2319–2329, 2004.
6. Ma, SP and Zahalak, GI. A distribution-moment model of energetics in skeletal muscle. *J Biomech* 24: 21–35, 1991.
7. McGill, SM. *Ultimate Back Fitness and Performance.* Waterloo, Canada: Backfitpro.com, 2006.
8. McGill, SM. *Low Back Disorders: Evidence Based Prevention and Rehabilitation.* (2nd ed.). Champaign: Human Kinetics Publishers, 2007.
9. McGill, SM, Childs, A, and Liebenson, C. Endurance times for stabilization exercises: clinical targets for testing and training from a normal database. *Arch Phys Med Rehabil* 80: 941–944, 1999.
10. Potvin, JR and Brown, SHM. An equation to calculate individual muscle contributions to joint stability. *J Biomech* 38: 973–980, 2005.
11. Waller, M, Piper, T, and Townsend, R. Strongman events and strength and conditioning programs. *Strength Cond J* 25: 44–52, 2003.